X chromosome and autosomal recombination are differentially sensitive to disruptions in SC maintenance

Katherine Kretovich Billmyre[a,1], Cori K. Cahoon[a,b,c,1], G. Matthew Heenan[a,d], Emily R. Wesley[a,e], Zulin Yu[a], Jay R. Unruh[a], Satomi Takeo[f], and R. Scott Hawley[a,d,2]

[a]Stowers Institute for Medical Research, Kansas City, MO 64110; [b]Institute of Molecular Biology, University of Oregon, Eugene, OR 97403; [c]Department of Biology, University of Oregon, Eugene, OR 97403; [d]Department of Molecular and Integrative Physiology, University of Kansas Medical Center, Kansas City, KS 66160; [e]University of Missouri–Kansas City, Kansas City, MO 64110; and [f]Department of Biological Sciences, Tokyo Metropolitan University, Tokyo, Japan 192-0397

Contributed by R. Scott Hawley, September 3, 2019 (sent for review June 25, 2019; reviewed by Monica P. Colaiacovo and Dean S. Dawson)

The synaptonemal complex (SC) is a conserved meiotic structure that regulates the repair of double-strand breaks (DSBs) into crossovers or gene conversions. The removal of any central-region SC component, such as the *Drosophila melanogaster* transverse filament protein C(3)G, causes a complete loss of SC structure and crossovers. To better understand the role of the SC in meiosis, we used CRISPR/Cas9 to construct 3 in-frame deletions within the predicted coiled-coil region of the C(3)G protein. Since these 3 deletion mutations disrupt SC maintenance at different times during pachytene and exhibit distinct defects in key meiotic processes, they allow us to define the stages of pachytene when the SC is necessary for homolog pairing and recombination during pachytene. Our studies demonstrate that the *X* chromosome and the autosomes display substantially different defects in pairing and recombination when SC structure is disrupted, suggesting that the *X* chromosome is potentially regulated differently from the autosomes.

synaptonemal complex | meiosis | homologous recombination | *Drosophila*

Several facets of meiosis ensure the faithful inheritance of chromosomes from parents to offspring. During the creation of eggs and sperm the genome must be reduced to a haploid state containing a single set of chromosomes. The failure to properly segregate chromosomes results in gametes with an incorrect number of chromosomes. Indeed, errors in meiotic chromosome segregation are the leading cause of miscarriage and aneuploidy in humans, which can result in chromosomal disorders such as Down syndrome and Turner syndrome (reviewed in ref. 1).

Proper segregation of chromosomes during meiosis relies on the formation of programmed double-strand breaks (DSBs), which are initiated by the evolutionarily conserved type II DNA topoisomerase-like protein Spo11 (Mei-W68 in *Drosophila*) (2, 3). These DSBs are then repaired as crossover or gene conversion events (Fig. 1 *A* and *B*). Crossovers mature into chiasmata (for a more detailed review of chiasmata in *Drosophila*, see ref. 4), which physically hold homologous chromosomes together from nuclear envelope breakdown until homolog separation at anaphase I, thus ensuring proper segregation of chromosomes (5). The placement of crossover events is highly nonrandom and is strictly regulated by multiple processes (4). First, crossover interference prevents 2 crossovers from occurring in close proximity to each other (6). Second, crossovers are excluded from the heterochromatin. Third, as a result of the centromere effect, crossing over is also reduced in those euchromatic regions that lie in proximity to the centromeres (4). Finally, even within the medial and distal euchromatin, crossing over is substantially higher toward the middle of the chromosome arms (7). These constraints do not affect the frequency or distribution of gene conversion events, which appear to be randomly distributed throughout the euchromatin (8–10). Thus, the control of crossover distribution may act at the level of DSB fate choice, rather than in determining the position of DSBs.

Previous studies have demonstrated that the synaptonemal complex (SC), a large protein structure that forms between homologous chromosomes, plays a role in controlling crossover distribution (11–15). The SC is a highly conserved tripartite structure, with 2 lateral elements and a central region (Fig. 1*C*) (reviewed in refs. 16–18). The central region is composed of transverse filament and central element proteins, while the lateral element proteins connect the central region to the chromosome axes (Fig. 1*C*). The known proteins that make up the *Drosophila* central region include the main transverse filament protein C(3)G, the transverse filament-like protein Corolla, and the central element protein Corona (CONA) (19–21).

Work in *Caenorhabditis elegans* has shown that the SC functions to monitor crossover placement by preventing additional crossover designation in a region adjacent to an existing crossover precursor (11). Furthermore, there is evidence in *Saccharomyces cerevisiae* that Zip1, a transverse filament protein, has 2 separable functions—one in building the SC and the other in recombination (14, 15). Lastly, in rice, there is evidence that a

Significance

This study investigates the function of a large protein complex, the synaptonemal complex (SC), that is necessary for the tightly controlled processes of DNA double-strand break (DSB) formation/repair and chromosome segregation during meiosis. The repair of programmed DSBs made during meiosis results in the exchange of genetic information between chromosomes and their subsequent segregation away from each other to produce haploid gametes. Failure to properly regulate these processes can lead to chromosomal abnormalities. Here we report that premature loss of full-length SC impairs proper maintenance of chromosome pairing throughout early meiosis and leads to improper crossover placement. This work will help further our understanding of the role of the SC in the regulation of homologous pairing and recombination.

Author contributions: K.K.B., C.K.C., S.T., and R.S.H. designed research; K.K.B., C.K.C., G.M.H., E.R.W., Z.Y., and J.R.U. performed research; C.K.C., Z.Y., and J.R.U. contributed new reagents/analytic tools; K.K.B., C.K.C., G.M.H., E.R.W., Z.Y., and J.R.U. analyzed data; and K.K.B., C.K.C., and R.S.H. wrote the paper.

Reviewers: M.P.C., Harvard Medical School; and D.S.D., Oklahoma Medical Research Foundation.

The authors declare no competing interest.

Data deposition: Original data underlying this paper have been deposited in the Stowers Original Data Repository, https://www.stowers.org/research/publications/libpb-1233.

[1]K.K.B. and C.K.C. contributed equally to this work.

[2]To whom correspondence may be addressed. Email: rsh@stowers.org.

This article contains supporting information online at www.pnas.org/lookup/suppl/doi:10.1073/pnas.1910840116/-/DCSupplemental.

First published September 30, 2019.

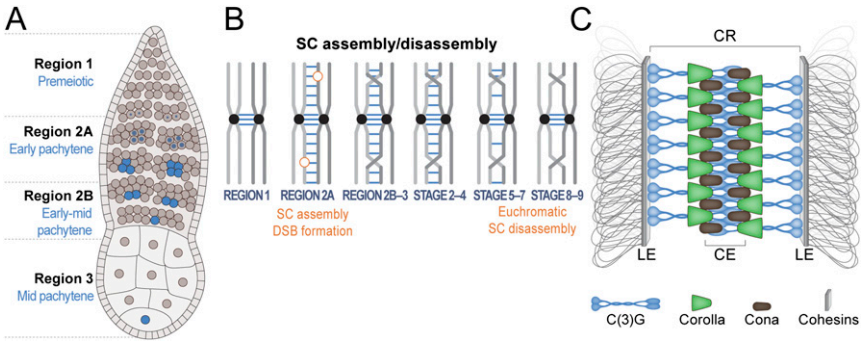

Fig. 1. Schematic of early meiosis in *Drosophila*. (*A*) Diagram of a *Drosophila* germarium and SC formation (described in ref. 4). At the anterior tip of the germarium, a germline stem cell divides asymmetrically to give rise to a cystoblast, which undergoes 4 mitotic divisions with incomplete cytokinesis to yield a 16-cell cyst. At region 2A (zygotene/early pachytene), up to 4 of the 16 cells in the cyst will enter meiosis and assemble the SC (represented by blue shading) to fully synapse the chromosomes. The oocyte selection process progresses in region 2B and is characterized by 2 nuclei (pro-oocytes) with a full-length SC (early to mid pachytene) and is completed by region 3 (mid pachytene) with only 1 oocyte per cyst retaining the full-length SC and all other nuclei having backed out of the meiotic program to become nurse cells. (*B*) Homologous chromosome pairing and SC assembly begin at the centromeres (represented as black dots on the chromosomes) during the mitotic divisions in region 1 (28, 29). In region 2A (early pachytene) the SC (represented by blue lines) is assembled along the chromosome arms and DSBs form (orange circles). The SC is maintained along chromosome arms until stages 5 to 7 (late pachytene), when SC disassembly occurs at multiple regions along the chromosome arms. The SC persists at the centromeres into stages 8 to 9 (mid prophase) (27, 47). (*C*) Model of the *Drosophila* SC showing the transverse filament protein C(3)G (blue), central-region (CR) protein Corolla (green), central element (CE) protein CONA (black), and lateral element (LE)/cohesin proteins (gray) connected to chromatin loops (adapted from ref. 4).

partial loss of the SC results in increased crossing over and crossover proximity similar to what was reported in *C. elegans* (11, 13). Based on what is known in other model systems, it is likely that the *Drosophila* SC is also playing a role in regulating the fate of DSBs and monitoring crossover placement.

In *Drosophila* females, ~24 DSBs are formed in early pachytene (22). Unlike in many other organisms where DSBs occur prior to SC formation, in *Drosophila* DSBs are formed in the context of fully formed SC (22–24) (reviewed in ref. 25). In the absence of the central region of the SC, DSB formation is substantially reduced, but not eliminated. Nonetheless, even in the presence of a substantial number of residual DSBs (37% of wild type), the loss of these SC proteins results in a complete loss of crossover formation (4, 19, 22, 26). The abolishment of the central region of the SC also results in a high frequency of unpaired homologs during pachytene (27–30). In addition to disrupting meiotic pairing, the loss of any of the known central-region components in the (premeiotic) mitotic region of the ovaries also impairs mitotic pairing of the second and third chromosomes (28).

Since the vast majority of SC mutants in *Drosophila* are null mutants and therefore fail to form any SC structure, it is difficult to investigate the interactions of the wild-type versions of these proteins at the protein level or discover how the SC is involved in DSB repair and fate choice. In *Drosophila*, the study of transgenes carrying in-frame deletions of either the N- or C-terminal globular domains of C(3)G has shown that both of these regions are required for proper SC assembly and crossover formation (31). However, these defects were too severe to allow us to investigate the function of the SC in crossover placement and formation. One domain which has not been tested is the large predicted coiled-coil domain in C(3)G. Coiled-coil domains are a key conserved feature of transverse filament proteins across many organisms and are known to be important for protein–protein interactions (32).

Here we characterize 3 in-frame deletion mutations in the coiled-coil domain of the *Drosophila melanogaster c(3)G*, all of which cause a partial loss of SC function at different stages in early meiosis. We take advantage of the different stages of SC loss to examine when the SC is necessary for multiple meiotic events such as pairing and recombination. Unlike any previously characterized *Drosophila* meiotic mutants (4, 33, 34), the effects of these mutants on *X* chromosome recombination is different from their effects on autosomal recombination. We infer from this observation that chromosomes can respond differently to a failure in SC maintenance. We also show that the SC in early pachytene is important for the maintenance of euchromatic pairing, especially in the distal euchromatin (in relation to the centromere) regions of the chromosome arms. The maintenance of *X* chromosome pairing is more sensitive to SC defects than is pairing maintenance on the autosomes, suggesting there may be additional chromosome-specific processes that mediate pairing. These mutants allowed us to examine the temporal requirement for the synaptonemal complex in crossover placement and maintenance of pairing.

Results

A 213-Amino Acid In-Frame Deletion within the Coiled-Coil Region of C(3)G Impairs the Maintenance of the SC in Early to Mid Pachytene. The 2 previous studies of the functional anatomy of C(3)G have relied on the analysis of transgenic constructs bearing in-frame deletions (21, 31). While extremely useful, transgenes have the disadvantage of nonendogenous expression levels and improper temporal expression. Based on previous studies in *S. cerevisiae* (35) and in *Drosophila* (21), CRISPR/Cas9 was employed to construct an in-frame deletion, $c(3)G^{cc\Delta 1}$, removing the base pairs encoding 213 amino acids (L340 to A552) from the 488-amino acid predicted coiled-coil domain of C(3)G (Fig. 2*A* and *SI Appendix*).

We first asked if $c(3)G^{cc\Delta 1}$ mutants retained the ability to assemble and disassemble the SC with normal kinetics. In wild-type flies, components of the central region of the SC are associated with paired centromeres during the premeiotic mitotic divisions (28, 29). By early pachytene these proteins are assembled as a tripartite SC that is visible as long, continuous tracks of Corolla and C(3)G (Fig. 2*B* and *SI Appendix*, Fig. S1). The SC remains fully assembled until mid to late pachytene (stages 5/7), at which point the SC is removed from the euchromatic chromosome arms but remains at the centromeres in mid pachytene (Fig. 1*B*) (reviewed in ref. 4). We assessed SC assembly in homozygous $c(3)G^{cc\Delta 1}$ females using a Corolla antibody to mark the central region of the SC. In early pachytene the total length of the SC was similar to wild type with a decrease in total SC length occurring in early to mid pachytene and a significant decrease in mid pachytene (Fig. 2 *B* and *C*; $P = 0.01$). However,

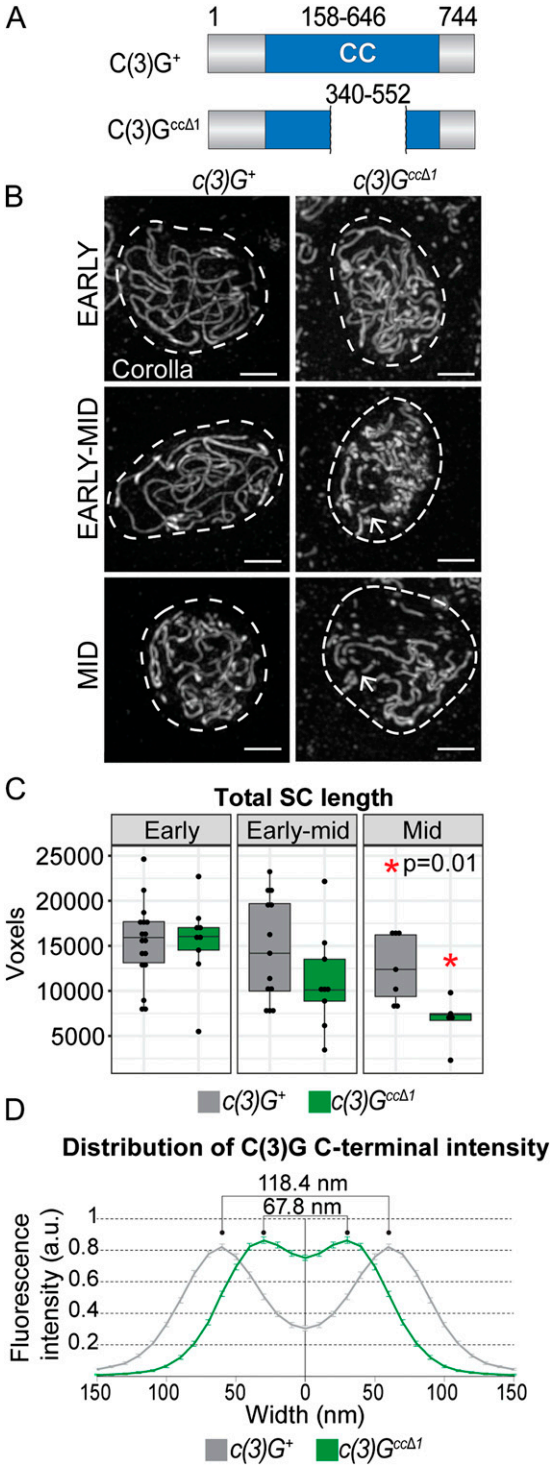

Fig. 2. In-frame deletion of part of the large coiled-coil region of C(3)G leads to a failure to maintain the SC. (*A*) The $c(3)G^{cc\Delta1}$ deletion removes the amino acids 340 to 552 from the coiled-coil (CC) domain of C(3)G. The predicted protein CC is in blue [based on COILS software (38)] and gray marks the unstructured region. (*B*) Images showing localization of the SC protein Corolla in $c(3)G^{+}$ and $c(3)G^{cc\Delta1}$ nuclei from early pachytene (region 2A) to mid pachytene (region 3). Dashed lines indicate the location of the nucleus as defined by DAPI staining (not shown). Arrows indicate discontinuities in the SC. (Scale bars, 2 μm.) (*C*) Quantification of the total track length of the C(3)G–positive SC in nuclei from early, early to mid, and mid pachytene using skeleton analysis (*SI Appendix*). *$P = 0.01$ by *t* test. $c(3)G^{+}$: $n = 17$ (early), $n = 13$ (early to mid), and $n = 7$ (mid); $c(3)G^{cc\Delta1}$: $n = 9$ (early), $n = 9$ (early to mid), and $n = 5$ (mid). (*D*) The average distribution of the distance between the 2 C-terminal C(3)G tracks is shown based on a line profile analysis of STED data in each genotype (*SI Appendix*). The quantification resulted in an average width of 118.4 ± 0.6 nm (SEM) in wild type and 67.8 ± 0.1 nm (SEM) in $c(3)G^{cc\Delta1}$ mutants. The average distribution was generated by averaging 46 line profiles from 8 wild-type nuclei and 35 line profiles from 12 $c(3)G^{cc\Delta1}$ nuclei.

the SC which formed in early to mid pachytene showed obvious discontinuities (Fig. 2*B*).

To determine whether or not the removal of a large region of the coiled-coil domain in $c(3)G^{cc\Delta1}$ mutants changed the tripartite structure of the SC, we measured the distance between the C termini of C(3)G. This was accomplished using a super-resolution technique, stimulated emission depletion (STED), in conjunction with a C(3)G C-terminal–specific antibody (19, 36). In wild-type controls the distance between the C termini of C(3)G was 118.4 nm (±0.6 nm SEM), while the distance in $c(3)G^{cc\Delta1}$ mutants was reduced to 67.8 nm (±0.1 nm SEM) (Fig. 2*D* and *SI Appendix*, Fig. S1). The decrease in SC width might be explained by the decreased length of C(3)G due to the 213 amino acids that were deleted. Since a single amino acid residue in a helix is predicted to be 0.15 nm in length (37), one would expect the decrease in length of a single $C(3)G^{cc\Delta1}$ homodimer to be 32 nm. Therefore, the width of the SC [which contains C(3)G homodimers arranged in a head-to-head orientation] would be predicted to be reduced by 64 nm in $c(3)G^{cc\Delta1}$ mutants. Although the observed 50-nm decrease in the width of the SC is less than predicted, the difference may be due to differences in the way that the $C(3)G^{cc\Delta1}$ homodimer interacts with the oppositely oriented homodimer emanating from the other lateral element. Most importantly, the reduction in coiled-coil length created by removal of a large portion of the coiled-coil domain does not disrupt the formation of the tripartite SC, as is illustrated by the 2 lateral tracks of C(3)G and the single track of Corolla observed using STED (Fig. 2*D* and *SI Appendix*, Fig. S1).

Loss of SC Maintenance in Early to Mid Pachytene Differentially Alters Crossing Over on the *X* Chromosome and Autosomes. The progressive (or temporal) loss of the SC in $c(3)G^{cc\Delta1}$ flies allowed us to determine whether or not the perdurance of full-length SC until early to mid pachytene was required for proper crossing over and/or crossover placement. We examined recombination on the *X* chromosome and found that the total amount of recombination along the entire chromosome was decreased from 63 to 11.8 cM (Fig. 3*A* and *SI Appendix*, Table S1). This reduction in exchange was clearly polar, a well-known attribute of recombination-deficient mutants in *Drosophila* (34). Specifically, the chromosomal region distal and medial to the centromere from *scute* (*sc*) to *vermillion* (*v*) exhibited a very low level of crossing over (3.7% of wild type), while the proximal euchromatin (in relation to the centromere) region from *v* to *yellow*$^{+}$ (y^{+}) was only reduced to 31.3% of wild type (Fig. 3*A* and *SI Appendix*, Table S1).

The analysis of crossing over on the second and third chromosomes did not reveal a reduction in total map length when comparing wild-type and $c(3)G^{cc\Delta1}$ flies (Fig. 3 *B* and *C* and *SI Appendix*, Tables S2 and S3). However, the pattern of exchange was again altered in a polar fashion, with a decrease in distal euchromatin recombination on both the second and third chromosomes (Fig. 3 *B* and *C* and *SI Appendix*, Tables S2 and S3; second, 59.6% of wild type; third, 58.2% of wild type) and a large increase (second, 319% of wild type; third, 447% of wild type) in the proximal euchromatin region (Fig. 3 *B* and *C* and *SI Appendix*, Tables S2 and S3). The greater than 300% increase in recombination across the proximal euchromatin region on both the second and third chromosomes suggests that normal, full-length SC in early to mid and mid pachytene is regulating,

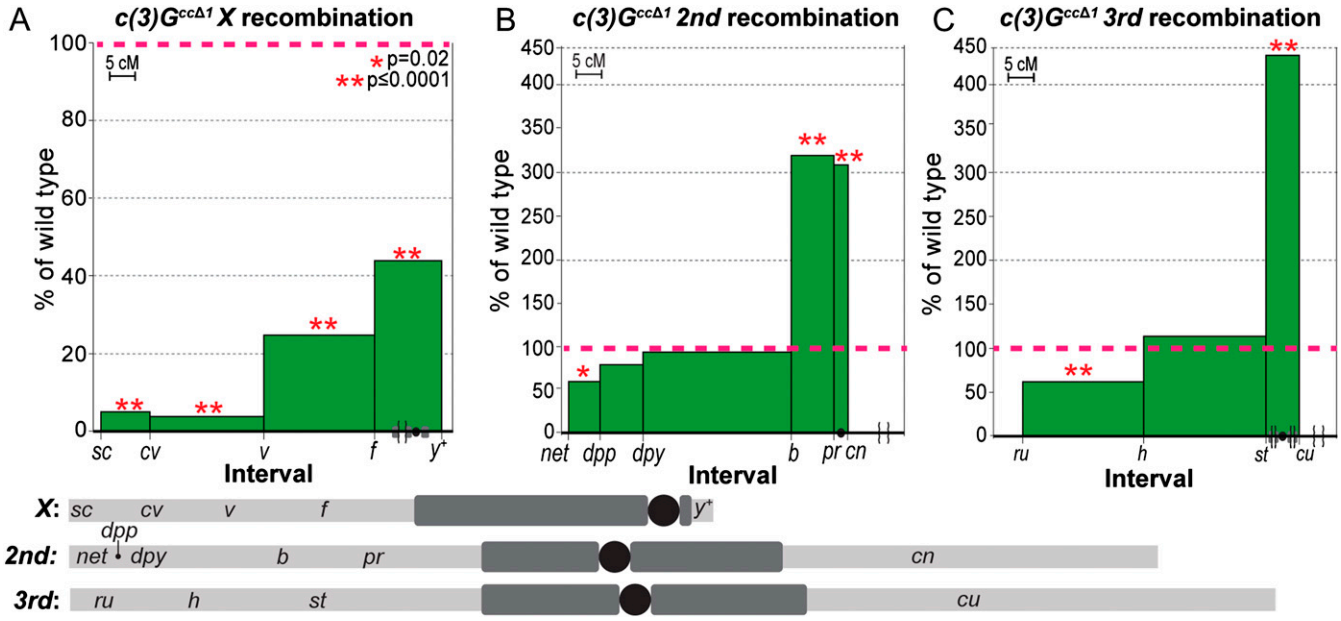

Fig. 3. *c(3)G*$^{cc\Delta 1}$ mutants exhibit chromosome-specific defects in recombination. Recombination in *c(3)G*$^{cc\Delta 1}$ females on the *X* chromosome (*A*), second chromosome (*B*), and third chromosome (*C*) is plotted with the percentage of wild type on the *y* axis vs. chromosome location (in cM) on the *x* axis. Brackets along the *x* axis indicate truncation of that region of the chromosome. The red dashed lines mark wild-type levels of recombination and are set at 100%. *P* values were obtained using a Fisher's exact test (*SI Appendix*, Tables S1–S3 for *N* values). See *SI Appendix* for the recessive markers used to assay recombination. For reference, below each chart is a diagram of the corresponding chromosome being analyzed displaying the relative cytological positions of the recombination markers and the approximate amounts of pericentromeric heterochromatin estimated from ref. 63 (the black circles represent the centromere).

directly or indirectly, crossover placement along the length of the chromosome.

The striking difference in recombination patterns between the *X* chromosome and autosomes suggests that the *X* chromosome responds differently to aberrations in the SC in early to mid pachytene than the autosomes. Such chromosome-specific defects in recombination have not been previously documented in *Drosophila* (4, 33). As discussed below, it is possible that the loss of the SC is not randomly distributed across all chromosomes and instead there is a loss of SC specifically on the *X* chromosome, causing a stronger recombination defect.

Smaller In-Frame Deletions within the Putative Coiled-Coil Domain Also Cause a Loss of SC Maintenance. One potentially confounding factor in the analysis of the *c(3)G*$^{cc\Delta 1}$ mutants was the decrease in the width of the SC (Fig. 2*D* and *SI Appendix*, Fig. S1) caused by the removal of a large region of the coiled-coil domain. The deletion of such a large region of the coiled coil could change the ability of the C(3)G protein to interact with itself and form a stable SC but it might also remove sites important for interacting with other proteins. Therefore, in an attempt to separate the multiple phenotypes seen in *c(3)G*$^{cc\Delta 1}$ flies, we created 2 smaller deletions within the larger deletion, *c(3)G*$^{cc\Delta 2}$ (D346 to T361) and *c(3)G*$^{cc\Delta 3}$ (K465 to V471) (Fig. 4*A*). These smaller regions should not significantly affect the length of the C(3)G protein based on the small number of amino acids deleted. These sites were picked based on regions of C(3)G where the COILS score (38) dipped, suggesting a loss of coiled-coil structure (*SI Appendix*, Fig. S2). We hypothesized these might be regions important for regulation of SC structure and/or function, independent of SC width.

When SC formation in *c(3)G*$^{cc\Delta 2}$ and *c(3)G*$^{cc\Delta 3}$ mutants was examined by Corolla staining, *c(3)G*$^{cc\Delta 2}$ flies displayed a similar SC length to wild type in early and early to mid pachytene but displayed a decrease in total SC length in mid pachytene when compared with wild type (Fig. 4 *B* and *C*; $P = 0.002$). However, *c(3)G*$^{cc\Delta 3}$ mutants never formed fully assembled full-length SC (Fig. 4 *B* and *C*; $P < 0.0001$). While both of these deletions are much smaller than the *c(3)G*$^{cc\Delta 1}$ deletion, they displayed different phenotypes. *c(3)G*$^{cc\Delta 2}$ mutants did not display a loss of SC length until mid pachytene, while *c(3)G*$^{cc\Delta 3}$ mutants had a more severe loss of SC in early pachytene compared with *c(3)G*$^{cc\Delta 1}$ mutants (Figs. 2*B* and 4*B*). We confirmed through antibody staining that the SC that did assemble in *c(3)G*$^{cc\Delta 2}$ and *c(3)G*$^{cc\Delta 3}$ mutants contained both C(3)G (*SI Appendix*, Fig. S2) and Corolla (Fig. 4*B*). The drastic differences in SC formation and maintenance observed in these mutants gave us a tool to examine the requirement of the SC in early pachytene vs. mid pachytene without the removal of a large structural region of C(3)G.

Full-Length SC in Mid Pachytene Is Not Necessary for X Recombination. When compared with *c(3)G*$^{cc\Delta 1}$ flies, the *c(3)G*$^{cc\Delta 2}$ mutants exhibited very different recombination phenotypes. First, *c(3)G*$^{cc\Delta 2}$ mutants had relatively normal levels of recombination along the *X* chromosome (109% of wild type; Fig. 5*A* and *SI Appendix*, Table S1) but still displayed increased proximal euchromatin recombination on the third chromosome in the *st*-to-*cu* interval (347% of wild type; Fig. 5*C* and *SI Appendix*, Table S3). Distal euchromatin recombination between *ru* and *h* on the third chromosome was reduced to 65.5% of wild-type levels in *c(3)G*$^{cc\Delta 2}$ (Fig. 5*C* and *SI Appendix*, Table S3).

In contrast to *c(3)G*$^{cc\Delta 2}$, the *c(3)G*$^{cc\Delta 3}$ deletion greatly reduced recombination on the *X* chromosome to 4.5% of wild type (Fig. 5*B* and *SI Appendix*, Table S1). This reduction was similar to, but more severe than, the reduction in X recombination seen in *c(3)G*$^{cc\Delta 1}$ mutants (18.7% of wild type; Fig. 3*A* and *SI Appendix*, Table S1). Additionally, *c(3)G*$^{cc\Delta 3}$ mutants mimicked the third chromosome recombination pattern we saw in *c(3)G*$^{cc\Delta 1}$ and *c(3)G*$^{cc\Delta 2}$ (Figs. 3*C* and 5*C* and *SI Appendix*, Table S3) with a distal euchromatin reduction and a large proximal euchromatin increase in recombination (Fig. 5*D*; distal, 25.5% of wild type; proximal, 404% of wild type). These large increases in proximal

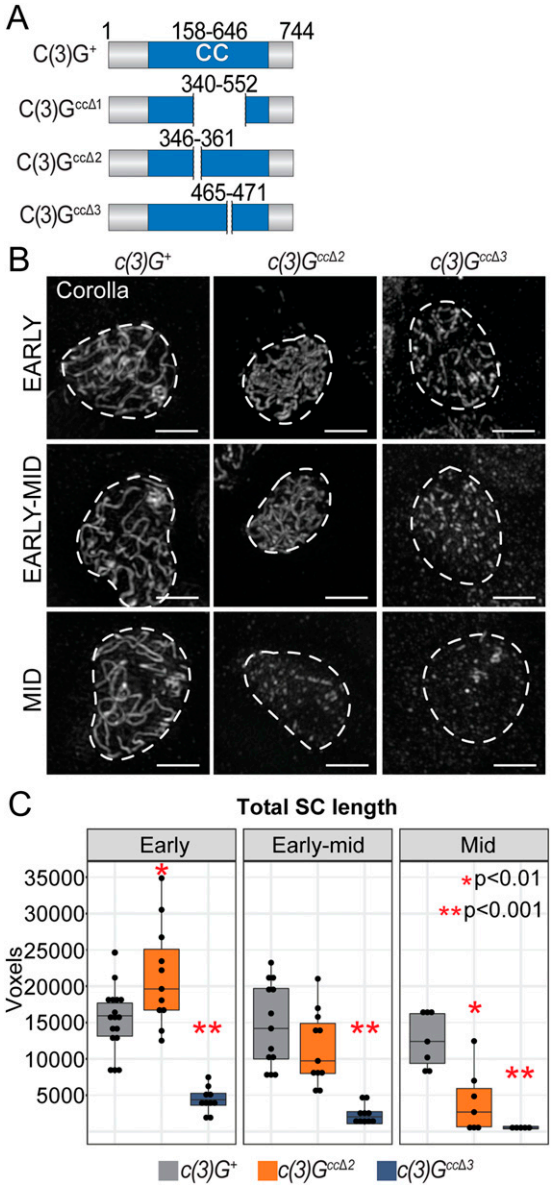

Fig. 4. Two smaller in-frame deletions within the putative *c(3)G* coiled-coil region cause varying levels of SC defects. (*A*) Diagrams of the C(3)G^{+}, C(3)G^{ccΔ1}, C(3)G^{ccΔ2}, and C(3)G^{ccΔ3} protein with the coiled-coil region marked in blue and the unstructured regions marked in gray. (*B*) Images showing localization of the SC protein Corolla in *c(3)G*$^{+}$, *c(3)G*^{ccΔ2}, and *c(3)G*^{ccΔ3} mutants from early pachytene (region 2A) to mid pachytene (region 3). Dashed lines indicate the location of the nucleus as defined by DAPI staining (not shown). (Scale bars, 2 μm.) (*C*) Quantification of the total length of the C(3)G–positive SC in nuclei from early, early to mid, and mid pachytene using skeleton analysis (*SI Appendix*). *c(3)G*$^{+}$ controls are the same ones used in Fig. 2. *$P < 0.01$ and **$P < 0.001$ by *t* test. *c(3)G*^{ccΔ2}: $n = 11$ (early), $n = 11$ (early to mid), and $n = 7$ (mid); *c(3)G*^{ccΔ3}: $n = 10$ (early), $n = 10$ (early to mid), and $n = 5$ (mid).

exchange parallel those observed in *c(3)G*^{ccΔ1} mutants for both the second and third chromosomes. We note that in all cases the mutant and control crosses carry identical pericentromeric regions and therefore the observed effects on exchange in the proximal euchromatin regions of the autosomes cannot be attributed to unrelated structural changes (*SI Appendix*, *Nondisjunction and Recombination Assays*).

To determine whether or not the *c(3)G*^{ccΔ3} deletion was dominant, we examined recombination on the *X* chromosome and the third chromosome in *c(3)G*^{ccΔ3}/+ heterozygotes. We found that the recombination pattern in the heterozygotes was similar to wild type, showing that the *c(3)G*^{ccΔ3} deletion does not display dominant effects on recombination (*SI Appendix*, Tables S1 and S3).

Alterations in Spo11-Dependent DSB Levels Are Not Responsible for Decreased Crossover Formation in *c(3)G*^{ccΔ1}, *c(3)G*^{ccΔ2}, and *c(3)G*^{ccΔ3} Mutants. To confirm that the decreases in *X* chromosome recombination observed in both the *c(3)G*^{ccΔ1} and *c(3)G*^{ccΔ3} mutants were not due to a large decrease in the formation of DSBs, we assessed DSB formation using γH2AV, a phosphorylated form of the histone variant H2AV that specifically marks sites of DSBs. Although both *c(3)G*^{ccΔ1} and *c(3)G*^{ccΔ3} flies exhibited normal kinetics for DSB repair from early to mid pachytene, *c(3)G*^{ccΔ1} flies [but not *c(3)G*^{ccΔ3} flies] displayed a decrease in the number of DSBs formed in early pachytene (*SI Appendix*, Fig. S3; $P = 0.03$). Since *X* chromosome recombination was more

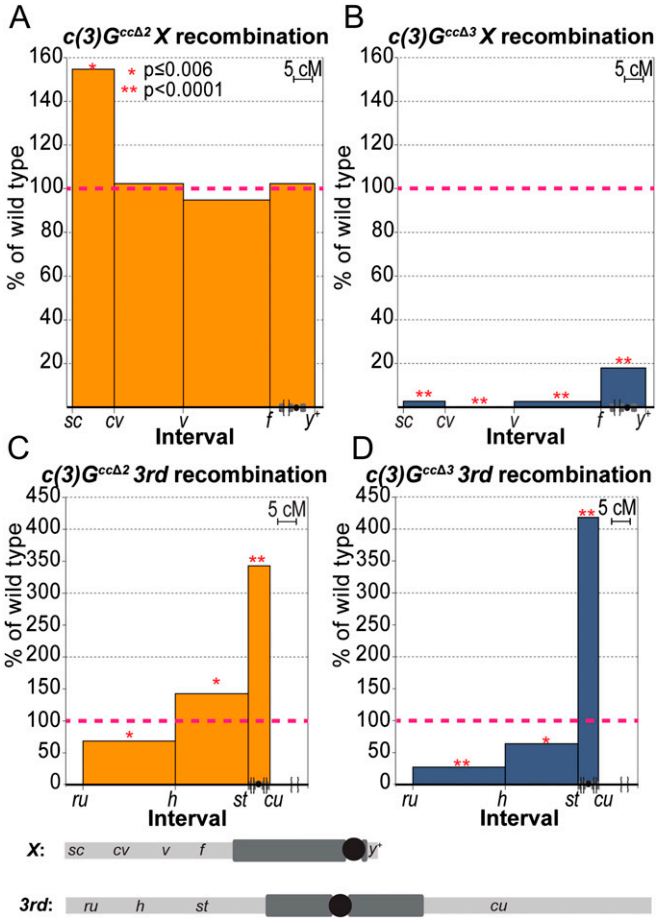

Fig. 5. Loss of SC maintenance in *c(3)G*^{ccΔ2} mutants in mid pachytene is not sufficient to disrupt *X* chromosome recombination. Recombination in *c(3)G*^{ccΔ2} and *c(3)G*^{ccΔ3} females on the *X* chromosome (*A* and *B*) and the third chromosome (*C* and *D*) is plotted with the percentage of wild type on the *y* axis vs. chromosome location (in cM) on the *x* axis. Brackets along the *x* axis indicate truncation of that region of the chromosome. The red dashed lines mark wild-type levels of recombination and is set at 100%. *P* values were obtained using a Fisher's exact test (see *SI Appendix*, Tables S1 and S3 for *N* values). See *SI Appendix* for the recessive markers used to assay recombination. For reference, below each chart is a diagram of the corresponding chromosome being analyzed displaying the relative cytological positions of the recombination markers and the approximate amounts of pericentromeric heterochromatin estimated from ref. 63 (the black circles represent the centromere).

severely affected in $c(3)G^{cc\Delta 3}$ flies compared with $c(3)G^{cc\Delta 1}$ flies, we do not believe the early pachytene decrease in $c(3)G^{cc\Delta 1}$ mutants is biologically relevant to the decrease in crossing over on the *X* chromosome. Lastly, we assessed DSB formation in $c(3)G^{cc\Delta 2}$ flies and saw a slight decrease in the number of DSBs formed in early pachytene compared with wild type (*SI Appendix*, Fig. S3; $P = 0.006$). However, $c(3)G^{cc\Delta 2}$ flies did not have an overall decrease in the formation of crossovers, and thus the decrease in γH2AV may not be biologically significant.

One possible explanation for the increase in proximal euchromatin recombination might be the induction of ectopic DSBs within the heterochromatin that were not induced by Spo11. To confirm that the proximal euchromatin recombination was due to Spo11 breaks, we constructed a double mutant with $c(3)G^{cc\Delta 3}$ and $vilya^{826}$, a recombination nodule component that is necessary for the induction of Spo11-induced breaks (39). When we assessed third chromosome recombination, we saw very low levels of recombination (total map length 1.4 cM; *SI Appendix*, Fig. S3), similar to the recombination seen in $vilya^{826}$ alone (39). This confirmed that the crossovers in $c(3)G^{cc\Delta 3}$ mutants are due to programmed Spo11 DSBs and not an increase in DNA damage.

Only $c(3)G^{cc\Delta 3}$ Mutants Display Mild Chromosome Segregation Defects. All previously characterized mutants in *Drosophila* that are unable to form crossovers, or have a significant reduction in crossovers genome-wide, display high levels of both X and fourth chromosome nondisjunction (19, 21, 40–42). The high levels of *X* chromosome nondisjunction observed in these recombination-defective mutants involve the interactions between both non–crossover *X* chromosomes and non–crossover autosomes (4, 34), such that 2 *X* chromosomes segregate from 1 autosome with the remaining autosomes segregating at random. In the absence of non–crossover autosomes, non–crossover *X* chromosomes will segregate normally. Additionally, in *Drosophila*, fourth chromosomes never undergo crossing over (i.e., the fourth chromosomes are obligately achiasmate). In wild-type flies with crossover second and third chromosomes, the non–crossover fourth chromosome segregates normally using a similar system as non–crossover *X* chromosomes (34).

When the rate of missegregation of the X and fourth chromosomes was assessed in all 3 mutants, neither $c(3)G^{cc\Delta 1}$ nor $c(3)G^{cc\Delta 2}$ mutants showed significantly increased levels of X or fourth chromosome nondisjunction when compared with wild type (*SI Appendix*, Table S4). $c(3)G^{cc\Delta 3}$ mutants displayed low levels of X (4.5%) and fourth (2.0%) chromosome nondisjunction (*SI Appendix*, Table S4). However, this low level of nondisjunction is much lower than the 39.2% reported in *c(3)G*-null mutants where the SC is completely absent (43).

The absence of an observed increase in *X* chromosome nondisjunction in $c(3)G^{cc\Delta 1}$ and $c(3)G^{cc\Delta 2}$ mutants is most likely explained by the absence of the nonexchange autosomes required to induce *X* chromosome nondisjunction. However, the low levels of X nondisjunction observed in $c(3)G^{cc\Delta 3}$ mutants might also be compatible with a proposed role for C(3)G-like proteins in mediating achiasmate segregations (44, 45). Therefore, the severe SC fragmentation present in $c(3)G^{cc\Delta 3}$ mutants may cause a mild segregation defect even in the presence of autosomal recombination.

The Loss of Full-Length SC in These Mutants Parallels a Decrease in Euchromatic Homolog Pairing. In *Drosophila*, homolog pairing is reduced in mutants lacking the SC (20, 30, 46). Thus, since our mutants exhibit SC defects in early to mid pachytene, we utilized them to investigate the importance of full-length SC in the maintenance of homolog pairing in *Drosophila*. Fluorescence in situ hybridization (FISH) was used to examine homologous pairing and to mark the distal and proximal euchromatic loci of the *X* chromosome.

In wild type, 90 to 100% of the *X* chromosome was paired from early to mid pachytene (Fig. 6*A*). To determine what the baseline level of pairing is in the absence of the SC, *X* chromosome pairing was assessed in females homozygous for a null allele of *c(3)G* [$c(3)G^{68}$]. In this genotype, the distal euchromatin region of the chromosome was most affected, with an average of 37% paired between early and early to mid pachytene, while the proximal euchromatin region was paired in about half the nuclei (Fig. 6*A*; 51.5%).

Starting at early to mid pachytene, $c(3)G^{cc\Delta 2}$ mutants exhibited a slight pairing defect at the distal euchromatin locus of the *X* chromosome (Fig. 6*A*; early, 90.9%; early to mid pachytene, 75%; mid pachytene, 58.8%) but were relatively well paired at the proximal euchromatin locus (Fig. 6*A*; early, 93.9%; early to mid pachytene, 95%; mid pachytene, 88.2%). Both $c(3)G^{cc\Delta 1}$ and $c(3)G^{cc\Delta 3}$ mutants displayed a progressive loss of pairing at both proximal and distal loci on the *X* chromosome. $c(3)G^{cc\Delta 1}$ mutants had almost a complete loss of distal pairing by mid pachytene, while $c(3)G^{cc\Delta 3}$ mutants only maintained 26% pairing (Fig. 6*A*).

These abnormalities in pairing maintenance correspond well with the recombination pattern seen on the *X* chromosome in $c(3)G^{cc\Delta 1}$ and $c(3)G^{cc\Delta 3}$ mutants in the sense that the distal region of the *X* chromosome was more affected than the proximal regions (Figs. 3*A* and 6*A*). The distal euchromatin decrease in recombination on the third chromosome in $c(3)G^{cc\Delta 1}$ and $c(3)G^{cc\Delta 3}$ mutants is displayed in conjunction with a similar loss of pairing. We examined pairing at distal, medial, and proximal euchromatic loci on the third chromosome throughout pachytene. Similar to the *X* chromosome, both $c(3)G^{cc\Delta 1}$ and $c(3)G^{cc\Delta 3}$ mutants displayed a similar trend of reduced pairing of the third chromosome, with a progressive decrease in distal euchromatin pairing that mirrors the recombination data (Fig. 6*B*). The medial and proximal regions of the third chromosome remained relatively paired from early to mid pachytene (Fig. 6*B*). It should be noted that in *c(3)G*–null mutants, pairing on the third chromosome was more strongly reduced; however, the proximal region (45% paired) was still paired more frequently than was the distal region (35% paired) (Fig. 6*B*).

To confirm that the loss of distal pairing on the third chromosome observed in $c(3)G^{cc\Delta 1}$ and $c(3)G^{cc\Delta 3}$ mutants was representative of the autosomes, we also examined pairing on the second chromosome in $c(3)G^{cc\Delta 1}$ mutants. Pairing on the second chromosome mirrored that of the third chromosome with a progressive loss of distal pairing but very little effect on medial and proximal pairing (*SI Appendix*, Fig. S4). The significant loss of distal pairing might explain why there are stronger recombination defects in the distal regions of both the X and third chromosomes in $c(3)G^{cc\Delta 1}$ and $c(3)G^{cc\Delta 3}$ flies. By the same reasoning, the autosomal pairing that is maintained in these mutants is in the proximal euchromatin region, which may allow for an increased number of recombination events that are within this proximal euchromatin.

Centromere Pairing Is Normal in $c(3)G^{cc\Delta 1}$, $c(3)G^{cc\Delta 2}$, and $c(3)G^{cc\Delta 3}$ Mutants but $c(3)G^{cc\Delta 3}$ Mutants Exhibit Centromere Clustering Defects. In wild-type *Drosophila* females, the 8 centromeres (2 for each of the 4 chromosomes) progressively pair in the premeiotic cysts, becoming 4 pairs of centromeres (which can be visualized as 4 foci). The paired centromeres then cluster into an average of 2 foci by early pachytene (27). The SC is important for centromere clustering in early meiotic cells with an average of 4 centromere foci in *c(3)G*-, *cona*-, and *corolla*-null mutants, indicating the presence of paired centromeres that are not clustered (19, 27, 47). Using an antibody against CID, a centromere-specific histone, we assessed if centromere clustering was altered in the context of SC loss in early to mid pachytene.

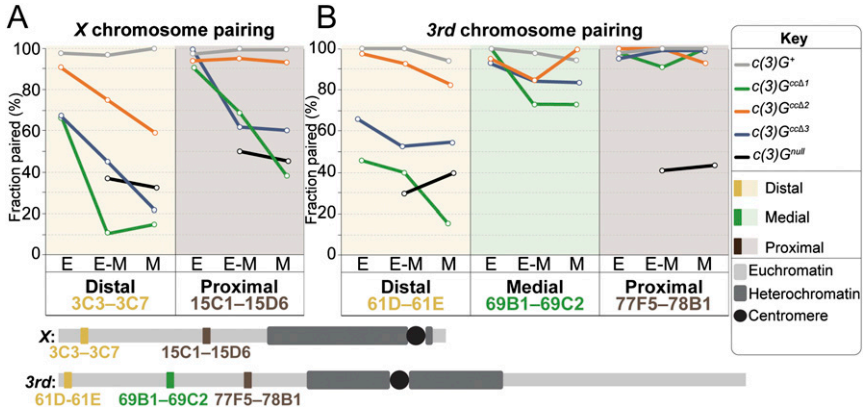

Fig. 6. SC in early to mid pachytene maintains homologous chromosome pairing. Fraction of paired euchromatic regions in $c(3)G^{+}$ controls (gray lines), $c(3)G^{ccΔ1}$ (green lines), $c(3)G^{ccΔ2}$ (orange lines), $c(3)G^{ccΔ3}$ (blue lines), and $c(3)G^{null}$ flies (black lines) assessed by FISH using BAC probes against either distal or proximal euchromatin regions on the *X* chromosome (*A*) and distal, medial, or proximal euchromatin regions on the third chromosome (*B*) at early (E), early to mid (E-M), or mid (M) pachytene. Early pachytene is not assessed in $c(3)G^{null}$ flies due to the lack of an SC, which is the only marker to identify early pachytene nuclei. For reference, below each chart is a diagram of the corresponding chromosome being analyzed (the black circles represent the centromere). For *N* values, see *SI Appendix*, Table S5; for the distance between unpaired foci, see *SI Appendix*, Fig. S4 and Table S6.

Oocytes from wild-type, $c(3)G^{ccΔ1}$, and $c(3)G^{ccΔ2}$ flies contained an average of 1.7 to 2.5 foci in early to mid pachytene, indicating normal centromere pairing and clustering (*SI Appendix*, Fig. S5). $c(3)G^{ccΔ1}$ mutants did display significantly more foci than controls in early and mid pachytene (*SI Appendix*, Fig. S5; $P = 0.01$ and 0.002, respectively). However, in $c(3)G^{ccΔ1}$ the average was 2.5 foci instead of 4 foci, suggesting that the loss of the SC in this mutant at early to mid pachytene was not likely to be impacting centromere pairing in $c(3)G^{ccΔ1}$. $c(3)G^{ccΔ3}$ mutants had an average of 3.6 foci in all 3 stages (*SI Appendix*, Fig. S5; $P < 0.001$), suggesting that some defects in SC assembly at early pachytene may be sufficient to disrupt centromere clustering but not centromere pairing.

Discussion

The SC plays multiple roles during meiosis that illustrate its importance in ensuring the successful transmission of genetic information from one generation to the next, yet our knowledge of how the SC is involved in regulating meiotic processes, such as recombination and the maintenance of pairing, is limited due to the integral nature of each SC component. Here we report partial loss-of-function SC mutations in a central-region component in *Drosophila*. We use the different stages of SC loss found in these mutants to show there is a temporal requirement of the SC in the regulation of crossover number and placement on the *X* chromosome versus the autosomes (Fig. 7). Additionally, a full-length SC is important for maintaining euchromatic homolog pairing in distal euchromatic chromosomal regions.

Regulation of SC Assembly and Disassembly. Both the regulation of SC assembly and disassembly, and its maintenance after assembly, is poorly understood. Work in other organisms has shown that posttranslational modifications are important in SC structure and function. It is known that SUMOylation and N-terminal acetylation promote assembly of the SC while phosphorylation or dephosphorylation promote disassembly of the SC with modifications occurring on multiple SC proteins (12, 48–50). Thus far, no posttranslationally modified sites have been identified on C(3)G. However, it is likely that these sites do exist, and we speculate that sites promoting SC assembly, maintenance, and disassembly may be disrupted in these mutants.

Another possibility is that the deletions described here could destabilize protein–protein interaction sites between C(3)G and other central-region proteins, resulting in an unstable SC that is difficult to maintain. We note that the mutant with the smallest deletion, $c(3)G^{ccΔ3}$, exhibited the strongest SC defect. While this deletion was predicted to only disrupt a single coil, the best explanation for the more severe phenotype is that it actually disrupts the coiled coil. This may have caused a large disruption in the rest of the coiled-coil structure. In the future, it will be important to further dissect these domains to better understand the regulation of SC assembly and disassembly.

A Role for the SC in the Maintenance of Homolog Pairing. A surprising result from these studies was the ability of these deletions to allow the progressive loss of homologous euchromatic pairing

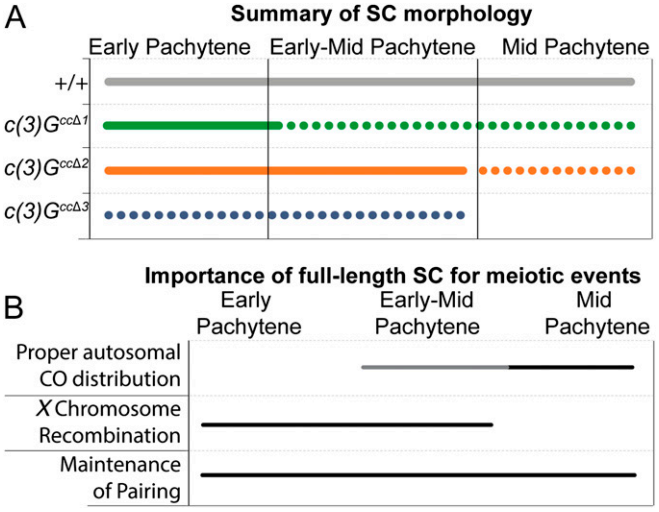

Fig. 7. Summary of SC morphology and model of the requirement for the SC in recombination and pairing maintenance. (*A*) Summary of SC phenotypes in $c(3)G^{+}$ (gray line), $c(3)G^{ccΔ1}$ (green line), $c(3)G^{ccΔ2}$ (orange line), and $c(3)G^{ccΔ3}$ (blue line) flies. $c(3)G^{ccΔ1}$ flies displayed SC defects in early to mid pachytene while $c(3)G^{ccΔ2}$ flies lost the SC in mid pachytene. $c(3)G^{ccΔ3}$ flies never fully assembled the SC. Dotted lines indicate defects in total SC length and fragmentation. (*B*) A model of the requirement of full-length SC (black lines) at different stages of pachytene. Based on our data, we propose that a full-length SC is important for proper autosomal crossover (CO) placement, *X* chromosome recombination, and maintenance of pairing at different stages of early to mid pachytene. The gray line represents a potential role for a full-length SC that cannot be confirmed with our data.

through pachytene. The mechanism behind establishing and maintaining homolog pairing is a long-standing, unanswered question in the meiosis field. Previous work in *Drosophila* has shown that in the complete absence of the central-region proteins C(3)G and CONA, euchromatic pairing is significantly reduced in early to mid and mid pachytene (20, 30, 46).

Our partial loss-of-function mutations have allowed us to test the importance of C(3)G in maintaining pairing throughout pachytene when the SC is present in early pachytene (unlike previous studies of null mutants in which the SC is always absent). From these mutants, we now have a timeline of when the SC is necessary to maintain pairing and recombination on the *X* chromosome and the autosomes. By comparing these mutants, we can hypothesize that the *X* chromosome needs a full-length SC earlier in pachytene for proper maintenance of pairing and recombination while the autosomes are likely capable of placing crossovers as late as mid pachytene, resulting in a proximal euchromatin shift in crossovers where pairing is maintained (Fig. 7).

In both $c(3)G^{cc\Delta 1}$ and $c(3)G^{cc\Delta 3}$ mutants, distal pairing of the *X* chromosome and the autosomes was most strongly reduced. One likely explanation for this stronger effect on distal regions of the chromosome arms is that normally the disassembly of the SC is initiated on the euchromatic chromosome arms with the centromeric region being removed last. Since the loss of the SC in $c(3)G^{cc\Delta 1}$ and $c(3)G^{cc\Delta 3}$ mutants occurs in a manner similar to wild-type SC disassembly, the distal regions of the chromosome may be affected earlier and more strongly than the proximal euchromatin regions. The proximal euchromatin region contains a large amount of heterochromatin that could be mediating pairing interactions and stabilizing pairing in the absence of the SC (51). Furthermore, our examination of centromere pairing suggests that the centromeres are still paired (*SI Appendix*, Fig. S5) and could be facilitating the proximal euchromatic pairing. This idea is supported by the higher levels of proximal euchromatic pairing compared with distal pairing in $c(3)G^{null}$ (Fig. 6).

Finally, we speculate that the ability of the $c(3)G^{cc\Delta 1}$ mutants to exhibit a distal euchromatic pairing defect that is more severe than the defect seen in $c(3)G^{null}$ mutants results from the residual proximal crossovers that do form in $c(3)G^{cc\Delta 1}$ mutants. Previous work has shown that crossovers can preserve synapsis but only in their vicinity (52, 53). Perhaps the stresses that provoke separation become more concentrated on the distal regions that lack crossovers. For example, it is possible that the untethered distal regions could experience a higher mechanical stress due to nuclear movements than the pericentric regions containing a crossover. The lack of a strong pairing defect in $c(3)G^{cc\Delta 2}$ mutants is probably due to the persistence of a full-length SC until mid pachytene. Together, these data support a role for the SC in maintaining euchromatic pairing during early to mid prophase (Fig. 7).

What Causes the Increase in Proximal Euchromatin Recombination Events? The autosomal increase in proximal euchromatin crossovers displayed in these mutants mimics the interchromosomal effect (9, 54). The interchromosomal effect has been reported in flies that are heterozygous for chromosome aberrations that suppress exchange in trans to a wild-type chromosome (55). Thus, the absence of crossover formation on one chromosome promotes increased recombination on the other chromosomes, with more crossovers placed in the proximal euchromatin regions (9, 54). The mechanism that controls the interchromosomal effect in balancer heterozygotes is poorly understood. Additionally, the interchromosomal effect has been reported in *C. elegans* mutants with defective synapsis, further supporting this possibility (56). It is possible that the interchromosomal effect is partially responsible for the increase in proximal euchromatin crossovers in $c(3)G^{cc\Delta 1}$ and $c(3)G^{cc\Delta 3}$ mutants due to the loss of *X* chromosome recombination.

However, the interchromosomal effect cannot explain the increase in proximal euchromatin recombination in $c(3)G^{cc\Delta 2}$ mutants since X recombination appears normal. In theory, this phenotype could be explained by crossover homeostasis, which functions to control the number of crossovers so the appropriate number is placed (reviewed in ref. 57). In many organisms, when there is a deficit of crossovers by the end of early to mid pachytene, the cell will continue to place crossovers in alternative locations to maintain an appropriate number. Such a process could result in crossovers being placed later than normal, which could be an issue when the SC is breaking down prematurely and homolog pairing is lost. However, Mehrotra and McKim (22) provide evidence that crossover homeostasis is unlikely to occur in *Drosophila* females. It is unknown how much of a role the SC plays in the repair of DSBs into crossover versus non–crossover events. It is possible the SC must be present to interact with factors necessary for regulating the placement of crossovers. For example, Vilya, a pro–crossover factor, localizes to the SC and DSBs prior to being recruited to recombination nodules (39). If DSB repair on the autosomes does not occur until early to mid pachytene and the SC is necessary for the determination of a crossover fate, it follows that loss of the SC in the euchromatin would result in a shift of crossover formation toward proximal euchromatin regions where the SC may still be present. This mechanism could also be increasing proximal euchromatin recombination in $c(3)G^{cc\Delta 1}$ and $c(3)G^{cc\Delta 3}$ flies. Alternatively, SC-independent heterochromatic pairing may be holding the proximal euchromatin region in close proximity, allowing for crossing over in that region. In addition to interacting with pro–crossover factors, the SC may be interacting with a currently unknown protein which regulates crossover placement differently on the *X* chromosome versus the autosomes.

Why Is There a Difference between the *X* Chromosome and the Autosomes? This set of mutants represents a unique tool to investigate not only the temporal requirements of the SC but also the differences in crossover placement between the *X* chromosome and the autosomes. Since $c(3)G^{cc\Delta 2}$ mutants do not display defects in *X* chromosome recombination, we conclude that a full-length SC throughout early to mid pachytene is sufficient for *X* chromosome crossover placement but not for normal distribution of autosomal crossovers (Fig. 7). Examining autosomal recombination in all 3 mutants suggests that a full-length SC is necessary in mid pachytene for proper crossover distribution on the autosomes (Fig. 7). There are multiple explanations for the recombination differences between the *X* chromosome and the autosomes.

The first of these hypotheses is that there might exist a timing difference in either synapsis or crossover placement between the *X* chromosome and the autosomes. Work in *C. elegans* has provided evidence for timing differences between the sex chromosomes and the autosomes. For example, the *X* chromosome initiates premeiotic DNA replication later than the autosomes (58, 59). This could be significant, as replication timing has been shown to impact crossover designation in barley (60). Additionally, in *C. elegans*, the *X* chromosome and the autosomes pair at the same time, but synapsis of the *X* chromosome is delayed and the *X* chromosome has lower levels of DSB formation compared with the autosomes (58, 61). Thus, the timing of when each chromosome is fully synapsed could be critical to ensure normal crossover placement, and the premature disruption of synapsis may affect the activity of pro–crossover factors. For example, in *C. elegans*, the XND-1 protein is required for genome-wide crossover placement and is important for normal rates of DSBs on the *X* chromosome (62). Currently, it is unknown in *Drosophila* if there are differences in the timing of DSB repair or synapsis of the *X* chromosome as compared with the autosomes, and our data suggest this as a possibility.

A second, but not mutually exclusive, explanation for the differences between the chromosomes may be a structural one. The *X* chromosome is acrocentric (the centromere is near the end of

the chromosome), while the autosomes are both metacentric (the centromere is near the center of the chromosome) and, perhaps, these structural differences mean that the *X* chromosome is more sensitive to loss of the SC. Our data suggest that loss of SC maintenance disrupts the maintenance of euchromatic homolog pairing more severely on the *X* chromosome than on the autosomes. It is unknown if metacentric chromosomes are different in terms of synapsis and recombination as compared with acrocentric chromosomes, and further investigation is needed to determine if structural differences affect these processes.

It is clear from decades of research that the regulation of recombination requires many factors and precise timing. Here we show that the SC plays a vital role in maintaining homolog pairing and proper crossover distribution in *Drosophila* female meiosis. Many differences between sex chromosomes and autosomes have been documented in a multitude of organisms, and our data are consistent with these differences extending into the processes that control chromosome pairing and recombination. With this set of mutants, we have established a system to examine *X* chromosome and autosome biology in *Drosophila* meiosis that will allow future work to unravel the mechanism behind meiotic chromosomal differences.

Methods

Stocks. *Drosophila* stocks were maintained on standard food at 24 °C. Descriptions of genetic markers and chromosomes can be found at https://www.flybase.org/. Wild type refers to the genotype *y w;* $^{+/+}$*;* $^{+/+}$*;* $sv^{spa\text{-}pol}$, unless stated otherwise. *SI Appendix*, *Key Resource Table* contains a list of all of the fly stocks used in this manuscript.

Construction of CRISPR Stocks. See *SI Appendix* for detailed methods.

Nondisjunction and Recombination Assays. See *SI Appendix* for detailed methods.

Immunostaining of Whole-Mount Ovaries. Germarium preparation for whole-mount immunofluorescence was modified from the protocol described in ref. 39, with dissections performed in PBS with 0.1% Tween. See *SI Appendix* for detailed methods.

Fluorescence In Situ Hybridization. FISH probes were designed from bacterial artificial chromosomes (BACs) obtained from the Children's Hospital Oakland Research Institute (https://bacpacresources.org/library.php?id=30). FISH with immunohistochemistry was performed as previously described (28). See *SI Appendix* for detailed methods.

Imaging and Image Analysis. Except for the STED imaging, all images were acquired on an inverted DeltaVision microscopy system (GE Healthcare) with an Olympus 100× objective (UPlanSApo 100×, NA 1.40) and a high-resolution CCD camera or an Applied Precision OMX Blaze microscope equipped with a PCO Edge sCMOS camera. See *SI Appendix* for detailed methods.

Data and Software Availability. Original data underlying this manuscript can be accessed from the Stowers Original Data Repository at https://www.stowers.org/research/publications/libpb-1233. For data analysis, the custom ImageJ plugins used are available at https://research.stowers.org/imagejplugins/zipped_plugins.html.

ACKNOWLEDGMENTS. We thank Claudio Sunkel for antibodies, past and present members of the R.S.H. laboratory for helpful discussions and comments on this manuscript, and Angela Miller for editorial and figure preparation assistance. R.S.H. is an American Cancer Society Research Professor.

1. T. Hassold, H. Hall, P. Hunt, The origin of human aneuploidy: Where we have been, where we are going. *Hum. Mol. Genet.* **16**, R203–R208 (2007).
2. S. Keeney, C. N. Giroux, N. Kleckner, Meiosis-specific DNA double-strand breaks are catalyzed by Spo11, a member of a widely conserved protein family. *Cell* **88**, 375–384 (1997).
3. K. S. McKim, A. Hayashi-Hagihara, mei-W68 in *Drosophila melanogaster* encodes a Spo11 homolog: Evidence that the mechanism for initiating meiotic recombination is conserved. *Genes Dev.* **12**, 2932–2942 (1998).
4. S. E. Hughes, D. E. Miller, A. L. Miller, R. S. Hawley, Female meiosis: Synapsis, recombination, and segregation in *Drosophila melanogaster*. *Genetics* **208**, 875–908 (2018).
5. R. B. Nicklas, Chromosome segregation mechanisms. *Genetics* **78**, 205–213 (1974).
6. L. E. Berchowitz, G. P. Copenhaver, Genetic interference: Don't stand so close to me. *Curr. Genomics* **11**, 91–102 (2010).
7. P. Szauter, An analysis of regional constraints on exchange in *Drosophila melanogaster* using recombination-defective meiotic mutants. *Genetics* **106**, 45–71 (1984).
8. D. E. Miller *et al*., Whole-genome analysis of individual meiotic events in *Drosophila melanogaster* reveals that noncrossover gene conversions are insensitive to interference and the centromere effect. *Genetics* **203**, 159–171 (2016).
9. K. N. Crown, D. E. Miller, J. Sekelsky, R. S. Hawley, Local inversion heterozygosity alters recombination throughout the genome. *Curr. Biol.* **28**, 2984–2990.e3 (2018).
10. D. E. Miller *et al*., A whole-chromosome analysis of meiotic recombination in *Drosophila melanogaster*. *G3 (Bethesda)* **2**, 249–260 (2012).
11. D. E. Libuda, S. Uzawa, B. J. Meyer, A. M. Villeneuve, Meiotic chromosome structures constrain and respond to designation of crossover sites. *Nature* **502**, 703–706 (2013).
12. S. Nadarajan *et al*., Polo-like kinase-dependent phosphorylation of the synaptonemal complex protein SYP-4 regulates double-strand break formation through a negative feedback loop. *eLife* **6**, e23437 (2017).
13. K. Wang, C. Wang, Q. Liu, W. Liu, Y. Fu, Increasing the genetic recombination frequency by partial loss of function of the synaptonemal complex in rice. *Mol. Plant* **8**, 1295–1298 (2015).
14. K. Voelkel-Meiman, S.-Y. Cheng, S. J. Morehouse, A. J. MacQueen, Synaptonemal complex proteins of budding yeast define reciprocal roles in MutSγ-mediated crossover formation. *Genetics* **203**, 1091–1103 (2016).
15. A. Storlazzi, L. Xu, A. Schwacha, N. Kleckner, Synaptonemal complex (SC) component Zip1 plays a role in meiotic recombination independent of SC polymerization along the chromosomes. *Proc. Natl. Acad. Sci. U.S.A.* **93**, 9043–9048 (1996).
16. D. Zickler, N. Kleckner, Meiotic chromosomes: Integrating structure and function. *Annu. Rev. Genet.* **33**, 603–754 (1999).
17. D. Zickler, N. Kleckner, Recombination, pairing, and synapsis of homologs during meiosis. *Cold Spring Harb. Perspect. Biol.* **7**, a016626 (2015).
18. C. K. Cahoon, R. S. Hawley, Regulating the construction and demolition of the synaptonemal complex. *Nat. Struct. Mol. Biol.* **23**, 369–377 (2016).
19. K. A. Collins *et al*., Corolla is a novel protein that contributes to the architecture of the synaptonemal complex of *Drosophila*. *Genetics* **198**, 219–228 (2014).
20. S. L. Page *et al*., Corona is required for higher-order assembly of transverse filaments into full-length synaptonemal complex in *Drosophila* oocytes. *PLoS Genet.* **4**, e1000194 (2008).
21. S. L. Page, R. S. Hawley, c(3)G encodes a *Drosophila* synaptonemal complex protein. *Genes Dev.* **15**, 3130–3143 (2001).
22. S. Mehrotra, K. S. McKim, Temporal analysis of meiotic DNA double-strand break formation and repair in *Drosophila* females. *PLoS Genet.* **2**, e200 (2006).
23. C. M. Lake, J. K. Holsclaw, S. P. Bellendir, J. Sekelsky, R. S. Hawley, The development of a monoclonal antibody recognizing the *Drosophila melanogaster* phosphorylated histone H2A variant (γ-H2AV). *G3 (Bethesda)* **3**, 1539–1543 (2013).
24. D. L. Lindsley, L. Sandler, The genetic analysis of meiosis in female *Drosophila melanogaster*. *Philos. Trans. R. Soc. Lond. B Biol. Sci.* **277**, 295–312 (1977).
25. S. Keeney, Mechanism and control of meiotic recombination initiation. Curr. Top. Dev. Biol. **52**, 1–53 (2001).
26. S. L. Page *et al*., A germline clone screen for meiotic mutants in *Drosophila melanogaster*. *Fly (Austin)* **1**, 172–181 (2007).
27. S. Takeo, C. M. Lake, E. Morais-de-Sá, C. E. Sunkel, R. S. Hawley, Synaptonemal complex-dependent centromeric clustering and the initiation of synapsis in *Drosophila* oocytes. *Curr. Biol.* **21**, 1845–1851 (2011).
28. N. Christophorou, T. Rubin, J.-R. Huynh, Synaptonemal complex components promote centromere pairing in pre-meiotic germ cells. *PLoS Genet.* **9**, e1004012 (2013).
29. E. F. Joyce, N. Apostolopoulos, B. J. Beliveau, C. T. Wu, Germline progenitors escape the widespread phenomenon of homolog pairing during *Drosophila* development. *PLoS Genet.* **9**, e1004013 (2013).
30. D. Sherizen, J. K. Jang, R. Bhagat, N. Kato, K. S. McKim, Meiotic recombination in *Drosophila* females depends on chromosome continuity between genetically defined boundaries. *Genetics* **169**, 767–781 (2005).
31. J. K. Jeffress *et al*., The formation of the central element of the synaptonemal complex may occur by multiple mechanisms: The roles of the N- and C-terminal domains of the *Drosophila* C(3)G protein in mediating synapsis and recombination. *Genetics* **177**, 2445–2456 (2007).
32. A. N. Lupas, J. Bassler, Coiled coils—A model system for the 21st century. *Trends Biochem. Sci.* **42**, 130–140 (2017).
33. D. M. Parry, L. Sandler, The genetic identification of a heterochromatic segment on the X chromosome of *Drosophila melanogaster*. *Genetics* **77**, 535–539 (1974).
34. B. S. Baker, J. C. Hall, "Meiotic mutants: Genic control of meiotic recombination and chromosome segregation" in *The Genetics and Biology of Drosophila*, M. Ashburner and E. Novitski, Eds. (Academic Press, 1976), vol. 1a, pp. 351–434.
35. K. S. Tung, G. S. Roeder, Meiotic chromosome morphology and behavior in zip1 mutants of *Saccharomyces cerevisiae*. *Genetics* **149**, 817–832 (1998).
36. L. K. Anderson *et al*., Juxtaposition of C(2)M and the transverse filament protein C(3)G within the central region of *Drosophila* synaptonemal complex. *Proc. Natl. Acad. Sci. U.S.A.* **102**, 4482–4487 (2005).
37. P. M. Steinert, L. N. Marekov, R. D. B. Fraser, D. A. D. Parry, Keratin intermediate filament structure. Crosslinking studies yield quantitative information on molecular dimensions and mechanism of assembly. *J. Mol. Biol.* **230**, 436–452 (1993).

38. A. Lupas, M. Van Dyke, J. Stock, Predicting coiled coils from protein sequences. *Science* **252**, 1162–1164 (1991).
39. C. M. Lake *et al*., Vilya, a component of the recombination nodule, is required for meiotic double-strand break formation in *Drosophila*. *eLife* **4**, e08287 (2015).
40. R. Yan, B. D. McKee, The cohesion protein SOLO associates with SMC1 and is required for synapsis, recombination, homolog bias and cohesion and pairing of centromeres in *Drosophila* meiosis. *PLoS Genet.* **9**, e1003637 (2013).
41. B. Krishnan *et al*., *Sisters unbound* is required for meiotic centromeric cohesion in *Drosophila melanogaster*. *Genetics* **198**, 947–965 (2014).
42. E. A. Manheim, K. S. McKim, The synaptonemal complex component C(2)M regulates meiotic crossing over in *Drosophila*. *Curr. Biol.* **13**, 276–285 (2003).
43. J. C. Hall, Chromosome segregation influenced by two alleles of the meiotic mutant c(3)G in *Drosophila melanogaster*. *Genetics* **71**, 367–400 (1972).
44. M. N. Gladstone, D. Obeso, H. Chuong, D. S. Dawson, The synaptonemal complex protein Zip1 promotes bi-orientation of centromeres at meiosis I. *PLoS Genet.* **5**, e1000771 (2009).
45. L. Previato de Almeida *et al*., Shugoshin protects centromere pairing and promotes segregation of nonexchange partner chromosomes in meiosis. *Proc. Natl. Acad. Sci. U.S.A.* **116**, 9417–9422 (2019).
46. W. J. Gong, K. S. McKim, R. S. Hawley, All paired up with no place to go: Pairing, synapsis, and DSB formation in a balancer heterozygote. *PLoS Genet.* **1**, e67 (2005).
47. N. S. Tanneti, K. Landy, E. F. Joyce, K. S. McKim, A pathway for synapsis initiation during zygotene in *Drosophila* oocytes. *Curr. Biol.* **21**, 1852–1857 (2011).
48. A. Sato-Carlton, C. Nakamura-Tabuchi, S. K. Chartrand, T. Uchino, P. M. Carlton, Phosphorylation of the synaptonemal complex protein SYP-1 promotes meiotic chromosome segregation. *J. Cell Biol.* **217**, 555–570 (2018).
49. P. W. Jordan, J. Karppinen, M. A. Handel, Polo-like kinase is required for synaptonemal complex disassembly and phosphorylation in mouse spermatocytes. *J. Cell Sci.* **125**, 5061–5072 (2012).
50. J. Gao *et al*., N-terminal acetylation promotes synaptonemal complex assembly in *C. elegans*. *Genes Dev.* **30**, 2404–2416 (2016).
51. A. F. Dernburg *et al*., Meiotic recombination in *C. elegans* initiates by a conserved mechanism and is dispensable for homologous chromosome synapsis. *Cell* **94**, 387–398 (1998).
52. M. P. Maguire, Crossover frequencies within paracentric inversions in maize: The implications for homologue pairing models. *Genet. Res.* **46**, 273–278 (1985).
53. M. P. Maguire, R. W. Riess, The relationship of homologous synapsis and crossing over in a maize inversion. *Genetics* **137**, 281–288 (1994).
54. E. F. Joyce, K. S. McKim, *Drosophila* PCH2 is required for a pachytene checkpoint that monitors double-strand-break-independent events leading to meiotic crossover formation. *Genetics* **181**, 39–51 (2009).
55. J. Lucchesi, "Interchromosomal effects" in *The Genetics and Biology of* Drosophila, M. Ashburner and E. Novitski, Eds. (Academic Press, 1976), vol. 1a, pp. 315–329.
56. Q. Li *et al*., The tumor suppressor BRCA1-BARD1 complex localizes to the synaptonemal complex and regulates recombination under meiotic dysfunction in *Caenorhabditis elegans*. *PLoS Genet.* **14**, e1007701 (2018).
57. N. Hunter, Meiotic recombination: The essence of heredity. *Cold Spring Harb. Perspect. Biol.* **7**, a016618 (2015).
58. S. Mlynarczyk-Evans, A. M. Villeneuve, Time-course analysis of early meiotic prophase events informs mechanisms of homolog pairing and synapsis in *Caenorhabditis elegans*. *Genetics* **207**, 103–114 (2017).
59. A. Jaramillo-Lambert, M. Ellefson, A. M. Villeneuve, J. Engebrecht, Differential timing of S phases, X chromosome replication, and meiotic prophase in the *C. elegans* germ line. *Dev. Biol.* **308**, 206–221 (2007).
60. J. D. Higgins *et al*., Spatiotemporal asymmetry of the meiotic program underlies the predominantly distal distribution of meiotic crossovers in barley. *Plant Cell* **24**, 4096–4109 (2012).
61. J. Gao, H. M. Kim, A. E. Elia, S. J. Elledge, M. P. Colaiácovo, NatB domain-containing CRA-1 antagonizes hydrolase ACER-1 linking acetyl-CoA metabolism to the initiation of recombination during *C. elegans* meiosis. *PLoS Genet.* **11**, e1005029 (2015).
62. C. R. Wagner, L. Kuervers, D. L. Baillie, J. L. Yanowitz, xnd-1 regulates the global recombination landscape in *Caenorhabditis elegans*. *Nature* **467**, 839–843 (2010).
63. M. Ashburner, K. Golic, R. Hawley, "Chromosomes and position effect variegation" in Drosophila: *A Laboratory Handbook*, J. Inglis, Ed. (Cold Spring Harbor Laboratory Press, Cold Spring Harbor, NY, ed. 2, 2005), pp. 1038–1039.